A computational model on the modulation of mitogen-activated protein kinase (MAPK) and Akt pathways in heregulin-induced ErbB signalling

Mariko HATAKEYAMA*[1,2], Shuhei KIMURA*[1], Takashi NAKA†, Takuji KAWASAKI‡, Noriko YUMOTO*, Mio ICHIKAWA*, Jae-Hoon KIM*, Kazuki SAITO*, Mihoro SAEKI*, Mikako SHIROUZU*, Shigeyuki YOKOYAMA*§‖ and Akihiko KONAGAYA*

*RIKEN Genomic Sciences Center, 1-7-22 Suehirocho, Tsurumi-ku, Yokohama, Kanagawa 230-0045, Japan, †Department of Computer Science, Kyusyu Sangyo University, 2-3-1 Matsukadai, Higashi-ku, Fukuoka 813-8503, Japan, ‡Fuji Research Institute Corporation, 2-3 Kanda Nishikicho, Chiyoda-ku, Tokyo 101-8443, Japan, §Department of Biophysics and Biochemistry, Graduate School of Science, The University of Tokyo, 7-3-1 Hongo, Bunkyo-ku, Tokyo 113-0033, Japan, and ‖Cellular Signaling Laboratory and Structurome Group, RIKEN Harima Institute at SPring-8, 1-1-1 Kohto, Mikazuki-cho, Sayo, Hyogo 679-5148, Japan

ErbB tyrosine kinase receptors mediate mitogenic signal cascade by binding a variety of ligands and recruiting the different cassettes of adaptor proteins. In the present study, we examined heregulin (HRG)-induced signal transduction of ErbB4 receptor and found that the phosphatidylinositol 3′-kinase (PI3K)-Akt pathway negatively regulated the extracellular signal-regulated kinase (ERK) cascade by phosphorylating Raf-1 on Ser^{259}. As the time-course kinetics of Akt and ERK activities seemed to be transient and complex, we constructed a mathematical simulation model for HRG-induced ErbB4 receptor signalling to explain the dynamics of the regulation mechanism in this signal transduction cascade. The model reflected well the experimental results observed in HRG-induced ErbB4 cells and in other modes of growth hormone-induced cell signalling that involve Raf-Akt cross-talk. The model suggested that HRG signalling is regulated by protein phosphatase 2A as well as Raf-Akt cross-talk, and protein phosphatase 2A modulates the kinase activity in both the PI3K–Akt and MAPK (mitogen-activated protein kinase) pathways.

Key words: computer simulation, cross-talk, ErbB, heregulin, signal transduction.

INTRODUCTION

ErbB receptor tyrosine kinases play essential roles in cellular proliferation and differentiation, and their deregulated expression or mutation highly correlates with the incidence of certain types of human cancer [1–3]. The ErbB receptor family is composed of ErbB1 [epidermal growth factor receptor (EGFR)], ErbB2, ErbB3 and ErbB4. Among these receptors, the signalling pathway of EGFR has been extensively analysed and studied by experiments and mathematical modelling [4–7]. These ErbB proteins share several characteristic features, including conserved intrinsic tyrosine kinase domains and extracellular ligand-binding domains that are distinct from each other in their binding properties and affinities to several kinds of epidermal growth factor-like ligands. The binding of these ligands to ErbB receptors results in diverse biological outputs, such as different potency levels in cellular transformation *in vitro* [8–10]. Two of these four ErbB receptor proteins, EGFR and ErbB4, are capable of receiving extracellular ligands and transphosphorylating the receptor molecule to recruit corresponding signalling cassettes [11,12]. The other two, ErbB2 and ErbB3, are an orphan receptor and impaired kinase respectively and they transduce mitogenic signals only when they are overexpressed or co-expressed with the other ErbB receptors [1–3,11,12]. Although many efforts have been made to solve the EGFR signal transduction mechanism, little is known about ErbB4 receptor signalling.

Heregulin (HRG)-stimulated ErbB4 receptor has been known to interact with Src-homology and collagen domain protein (Shc) adaptor protein and p85 subunit of the phosphatidylinositol 3′-kinase (PI3K) [13,14]. Shc is known to recruit the growth factor receptor-binding protein 2 (Grb2)–Son of Sevenless homologue protein (Sos) complex (GS) before Ras association, and then activates the MAPK (mitogen-activated protein kinase) cascade. However, the downstream signalling cascade of PI3K has not been fully determined for HRG-induced ErbB4 receptor signalling. The membrane receptor association has been observed to activate PI3K, and the activated PI3K catalyses phosphatidylinositol (PI), resulting in the release of second messengers to activate protein kinase B/Akt in response to external growth hormones in several types of cell lines [15,16]. A number of recent studies further showed that PI3K-activated Akt phosphorylates Raf-1 on its Ser^{259} residue and thereby inhibits Raf-1 and the subsequent ERK activity [17–21]. In muscle cells, the Akt-induced inhibition of Raf-MEK-ERK pathway is stage-specific, and this cross-regulation depends on the state of cell differentiation [20]. Similarly, this kind of cross-inhibition is supposed to be ligand-specific in vascular smooth-muscle cells [22] or specific for high concentrations of insulin-like growth factor (IGF)-1-induced cellular signalling in MCF-7 cells [18].

In the present study, we examined how the PI3K-Akt pathway and its interference with the Raf-ERK pathway were involved in HRG-stimulated ErbB4 receptor signalling in Chinese-hamster

Abbreviations used: CHO, Chinese-hamster ovary; EGFR, epidermal growth factor receptor; ERK, extracellular signal-regulated kinase; ERKPP, phosphorylated ERK; Grb2, growth factor receptor-binding protein 2; HRG, heregulin; IGF, insulin-like growth factor; MAPK, mitogen-activated protein kinase; MEK, MAPK/ERK kinase; MEKPP, phosphorylated MEK; MKP3, MAPK phosphatase 3; PDK1, 3′-phosphoinositide-dependent kinase 1; PI, phosphatidylinositol; PI3K, phosphatidylinositol 3′-kinase; PIP_3, phosphatidylinositol-3,4,5-trisphosphate; PP2A, protein phosphatase 2A; Shc, Src-homology and collagen domain protein; Sos, Son of Sevenless homologue protein; GS, Grb2–Sos complex; ShGS, Shc-GS.

[1] These authors have contributed equally to this work.
[2] To whom correspondence should be addressed (e-mail marikoh@gsc.riken.go.jp).

ovary (CHO) cells that express ErbB4. As a result, we found that the addition of HRG induced rapid phosphorylation of Akt in ErbB4-expressing cells. Pretreatment of the cells with wortmannin, a PI3K inhibitor, abolished Akt phosphorylation under this condition, although it increased the phosphorylation of ERK to a level higher than that observed in the cells treated with HRG alone. In another study examining Ser^{259} phosphorylation of Raf-1, a basal level of phosphorylation of Ser^{259} was observed in the absence of HRG, and this phosphorylation was inhibited by the addition of wortmannin before HRG treatment. Thus Ser^{259} phosphorylation was considered to, at least partially, account for the PI3K-Akt pathway. These results have led us to the conclusion that PI3K-induced Akt activation suppresses the ERK pathway through the negative regulation of Raf-1.

Based on this observation, we developed a computer simulation model for the HRG-induced ErbB4 signalling pathway to understand the dynamics of the regulation of kinase activities in the system. To judge the validity of this model, we also analysed the pattern of ERK activation in response to the dephosphorylation of MEK and Akt by protein phosphatase 2A (PP2A) using the model with and without Raf-Akt cross-talk and PP2A regulation. In conclusion, the simulation results raised the possibility that HRG signalling is regulated by PP2A as well as Raf-Akt cross-talk as a means of modulating the kinase activities in both PI3K-Akt and Raf-MEK-ERK pathways. Furthermore, in our model, ERK and Akt showed maximum activity and behaved as if there were no cross-talk in the signalling cascades under certain conditions where the catalytic activity or the concentration of PP2A is very low. Thus the system behaviour in our model, which contains Raf-Akt cross-talk, is influenced significantly by the concentration and kinetic character of kinases and phosphatases. We therefore assume that such mechanisms may contribute to the cellular machinery for the induction of Raf-Akt cross-talk in ligand- or stage-specific signal transduction of cells.

EXPERIMENTAL

Materials

Recombinant human HRG-$\beta_{176-246}$ was purchased from R&D Systems (Minneapolis, MN, U.S.A.). Antibodies detecting phospho-p44/42 ERK, phospho-Ser^{473} Akt, phospho-Ser^{259} Raf-1, ERK and Akt were purchased from Cell Signaling Technology (Beverly, MA, U.S.A.). The specific antibodies used in detecting protein phosphorylation and protein interaction were obtained as follows: anti-ErbB4 receptor, anti-phosphotyrosine antibody (PY20) and anti-Raf-1 antibody from Santa Cruz Biotechnology (Santa Cruz, CA, U.S.A.); anti-p85 domain of PI3K from Upstate Biotechnology (Lake Placid, NY, U.S.A.); and anti-Shc antibody from Transduction Laboratories (Lexington, KY, U.S.A.). Wortmannin (PI3K inhibitor) and PD98059 (MEK inhibitor) were obtained from Calbiochem (San Diego, CA, U.S.A.). The method to construct CHO cells expressing human ErbB4 receptor has been described elsewhere [23].

Cell culture

CHO cells expressing ErbB4 receptor were routinely maintained in Dulbecco's modified Eagle's medium/F12 medium (Gibco BRL, Gaithersburg, MD, U.S.A.), supplemented with 10 % (v/v) bovine calf serum and antibiotics. For detection of the effect of HRG, the cells were starved in serum-free Dulbecco's modified Eagle's medium/F12 medium for 16–24 h before the experiment. To test the effect of wortmannin, the cells were pretreated with the inhibitor 10 min before the addition of HRG.

Western-blot analysis

HRG-stimulated cells were rinsed by ice-cold PBS and lysed with cell lysis buffer (1 % Triton X-100, 0.5 % deoxycholate, 0.1 % SDS, PBS and protease inhibitors; pH 7.4). The cell lysate was cleared by centrifugation, and the protein concentration of the supernatant was determined by Protein Assay Reagent (Bio-Rad Laboratories, Hercules, CA, U.S.A.). To detect and quantify the phosphorylated receptor in total ErbB4 receptor protein, cell lysate samples containing equal amounts of protein were immunoprecipitated using anti-ErbB4 antibody and anti-phosphotyrosine antibody (PY20) respectively, incubated once for at least 3 h at 4 °C and then incubated again with Protein A/G–agarose for 2 h at 4 °C. After extensive washing with PBS, the immunoprecipitate samples were resolved by SDS/PAGE side by side, and the resolved proteins were transferred to a PVDF membrane and blotted with anti-ErbB4 antibody. Protein bands were detected using chemiluminescent reagent (Santa Cruz Biotechnology), and the band intensity was quantified by a densitometer (Fuji-Film Corp., Tokyo, Japan). Alternatively, ErbB4 immunoprecipitates were detected with PY20 and then reblotted with anti-ErbB4 antibody. Anti-Shc and anti-p85 antibodies were used to detect the association of Shc and PI3K in the immunoprecipitated ErbB4 receptor. We examined ERK and Akt phosphorylation as downstream markers of Raf-MEK-ERK cascade and the PI3K-Akt pathway respectively. Given that Ser^{473} phosphorylation accounts for more than 90 % of enzymic activity of Akt, anti-phospho-Ser^{473} Akt antibody was used for the detection of the active form of Akt in the evaluation of Akt activity [24].

For the detection of phospho-p44/42 ERK and phospho-Ser^{473} Akt, equal amounts of protein were subjected to SDS/PAGE, the membrane was transferred, and the protein bands were then detected using the corresponding phospho-specific antibodies. Next, the membrane was treated in stripping buffer (Bio-Rad Laboratories) and reblotted with non-phospho-ERK or Akt antibodies. To estimate roughly the amount of active kinase in the total kinase protein, cell lysate was immunoprecipitated by anti-ERK (or anti-Akt) and anti-phospho-ERK (or anti-phospho-Akt) antibody, resolved by SDS/PAGE and stained with silver. Protein bands corresponding to the molecular mass of the proteins were quantified using a densitometer, and the ratio of phosphoproteins to the total proteins was calculated.

For the detection of phosphorylation of Raf-1 on Ser^{259}, cell lysates were immunoprecipitated with anti-phospho-Ser^{259} antibody (Cell Signaling Technology) and examined by Western blotting. Resolved bands were detected with the same antibody. An equal amount of the protein was subjected to Western blotting and detected by anti-Raf-1 antibody to judge the content of the protein corresponding to Raf-1.

Computation

To evaluate the dynamics of signal transduction pathways, we developed a stoichiometric simulation program YAGNS (Yet Another Gene Network Simulator), in our laboratory. The program solves the ordinary differential equations that are automatically formed from the inputs, and displays various time-course results in graphs. The inputs for the program include the reaction formula, kinetic parameters, initial concentrations of reactants and the simulation time. All computations for the present study

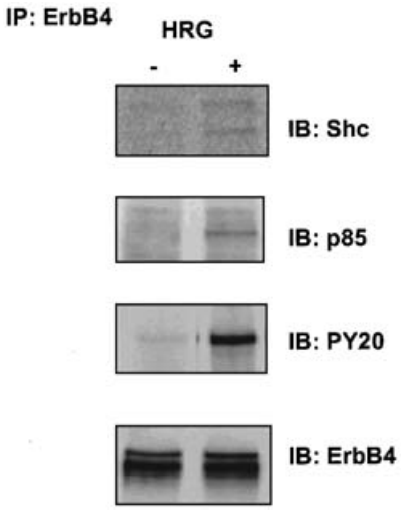

Figure 1 Association of Shc and p85 proteins with tyrosine-phosphorylated ErbB4 receptor after treatment of the ErbB4 cells with HRG

ErbB4-expressing cells were treated with 10 nM HRG for 2 min and the cell lysate (1 mg) was immunoprecipitated with anti-ErbB4 antibody. Samples were analysed by Western blotting with anti-Shc (the top panel), anti-PI3K p85 (the second panel), anti-phosphotyrosine (the third panel) and anti-ErbB4 (bottom panel) antibodies.

were performed on a Pentium III personal computer. The web interface version of this program is available at https://access.obigrid.org/.

To estimate unknown kinetic parameters and the concentrations of reactants, we developed a genetic algorithm called DIDC (Distance Independent Diversity Control). Parameter calculation was run on the PC cluster system (256CPU). This parameter estimation technique allows us to establish computer simulations of signal transduction pathways when kinetic parameters of the reactants are not obtained from laboratory experiments. The DIDC algorithm is described in Appendix A. This program is also available on the above website.

RESULTS

Raf-Akt cross-regulation in HRG signalling

To initiate the signal transduction pathways, a ligand-induced association of adaptor proteins with the activated and tyrosine-phosphorylated receptor is necessary. At first, we examined whether the p85 domain of PI3K and Shc could directly associate with HRG-activated ErbB4 receptor in our CHO cell line expressing ErbB4. In concordance with the results reported previously, we found that p85 and Shc directly interacted with the ErbB4 receptor immunoprecipitates after the addition of 10 nM HRG to the cells (Figure 1) [13,14]. Treatment of the cells with HRG induced a rapid Akt activation that reached a peak after 2 min and sustained phosphorylation for over 30 min (Figure 2A). Pretreatment of the cells with the PI3K inhibitor wortmannin completely inhibited this Akt phosphorylation. This confirmed that HRG activated Akt in a PI3K-dependent manner in the ErbB4-expressing cells. HRG also triggered ERK activation (Figure 2B). This activation was transient, and reached a peak 5–10 min after the addition of HRG. On the other hand, the cells pretreated with wortmannin showed a higher level of phosphorylated ERK than the cells treated with HRG alone. We repeated the same experiments three times and confirmed that the

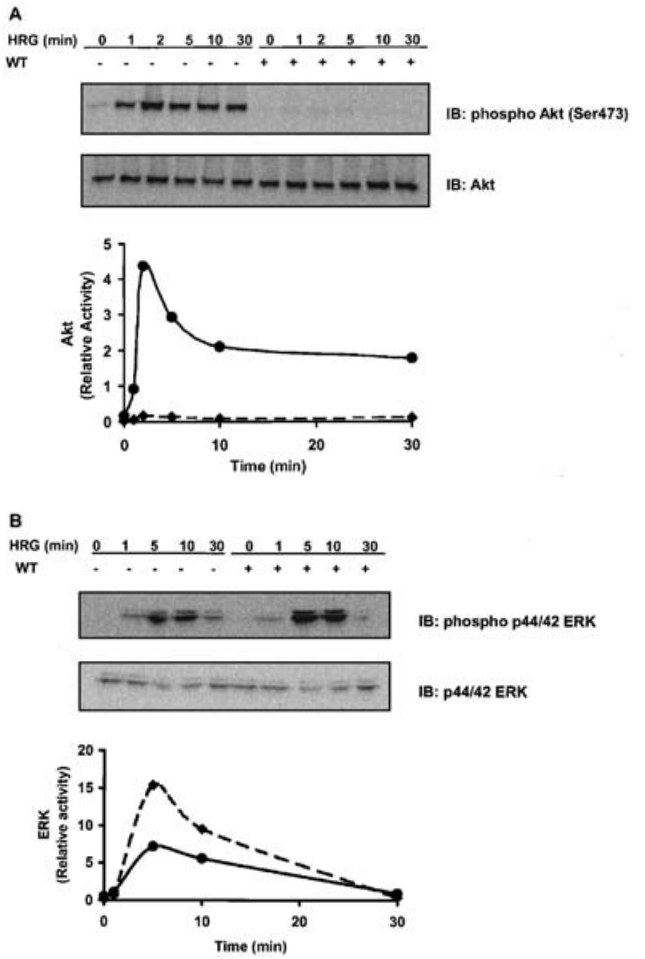

Figure 2 HRG-induced activation of Akt and ERK and the effect of the PI-3K inhibitor

Serum-starved ErbB4-expressing CHO cells were incubated with 10 nM HRG for the indicated times with or without pretreatment of 1 μM wortmannin. Phosphorylation of Ser^{473} Akt (**A**) and p44/42 ERK (**B**) in cell lysates (40 μg) was analysed by Western blotting using the corresponding anti-phospho-specific antibodies [(**A**), upper panel, anti-phospho-Ser^{473} Akt; (**B**), upper panel, anti-phospho-p44/42 ERK] and reblotted with anti-Akt or ERK antibodies [(**A**), lower panel, anti-Akt; (**B**), lower panel, anti-p44/42 ERK]. The graphs show densitometric quantification of phosphorylation of Akt and ERK after treatment of the cells with 10 nM HRG in the absence (broken line) or presence (solid line) of wortmannin (1 μM).

ERK phosphorylation was more extensive in the cells pretreated with wortmannin.

Akt is a serine/threonine kinase known to phosphorylate specifically proteins with the highly conserved peptide motif RXRXXS/T. The same motif is located in the Raf-1 N-terminal regulatory domain at Ser^{259} (RQRSTS). The potential ability of Akt to phosphorylate Raf-1 protein was first pointed out by bioinformatics analysis based on peptide library screening [25,26], and later it was proven experimentally *in vitro* [21]. Experimental studies have shown that a PI3K inhibitor inhibits the IGF-induced phosphorylation of Raf-1 on Ser^{259} and increases the extent of the kinase activities of Raf-1 and ERK in HEK-293 and MCF-7 cells. Later, the direct phosphorylation of Raf-1 on Ser^{259} by Akt was proven, and this Akt activity was confirmed to inhibit Raf-1 activity [18,21]. Thus the extent of Ser^{259} phosphorylation is critical for Raf-1 activity.

To confirm whether the PI-3K-Akt pathway is involved in the phosphorylation of Raf-1 on Ser^{259} in HRG-induced ErbB4

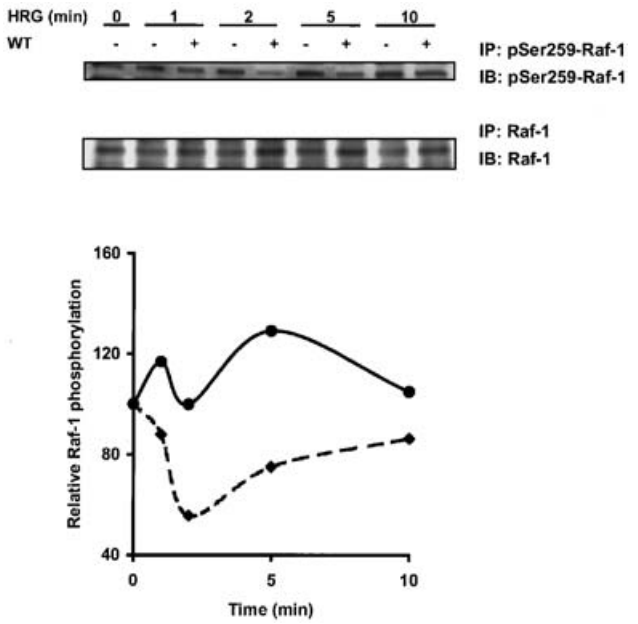

Figure 3 Phosphorylation of Raf-1 on Ser^{259} in HRG-treated ErbB4 cells

Cells were pretreated with 1 μM wortmannin before the addition of 10 nM HRG. The phosphorylated form of Raf-1 was immunoprecipitated by anti-phospho-Ser^{259} Raf-1 antibody from the lysate (500 μg) of ErbB4-expressing CHO cells and detected by the same antibody. Similarly, total Raf-1 protein was immunoprecipitated and detected by Raf-1 antibody. The graphs show densitometric quantification of phosphorylation of Raf-1 after treatment of the cells with 10 nM HRG in the absence (broken line) or presence (solid line) of 1 μM wortmannin.

signalling, we examined the phosphorylation of Raf-1 on Ser^{259} after HRG treatment in the presence or absence of wortmannin. Our results showed that Ser^{259} was constitutively phosphorylated, and this unphosphorylated form proved to be most remarkable at 2 min in the cells pretreated with wortmannin (Figure 3). Noting that this pattern of phosphorylation after wortmannin treatment inversely corresponded to the activity profile of Akt in our experiment (Figure 2A), we surmised that the Akt activity largely accounted for the Ser^{259} phosphorylation of Raf-1 at 2 min. At the same time, Akt-induced Ser^{259} phosphorylation remained low throughout the incubation time period, and most of the phosphorylation of Raf-1 on Ser^{259} seemed to depend on another kinase that is yet to be identified [17]. These results provided evidence that the PI3K-Akt pathway regulates Raf-1 activation in HRG-induced ErbB4 receptor signalling.

The signal transduction mechanism was assumed to be complex, commencing with the association of Shc and PI3K with the receptor after HRG binding and the consequent cross-regulation of ERK activity by the PI3K-Akt pathway. We organized the biochemical information on the regulatory mechanism of Akt on ERK and developed a mathematical simulation model for HRG signalling to analyse a signal transduction system involving Raf-MEK-ERK and PI3K-Akt pathways.

Description of ErbB4 model

The model is shown in Scheme 1. HRG-induced ErbB4 receptor bears two distinct signalling cassettes, the Ras-Raf-MEK-ERK and PI3K-Akt pathways. HRG binds to ErbB4 receptor ('R' in Scheme 1) and causes receptor dimerization, then the ErbB4 receptor kinase transphosphorylate each other at certain tyrosine residue sites in the receptor molecule ['RP' (a phosphorylated form of ErbB4 receptor)]. Phosphorylated ErbB4 possesses

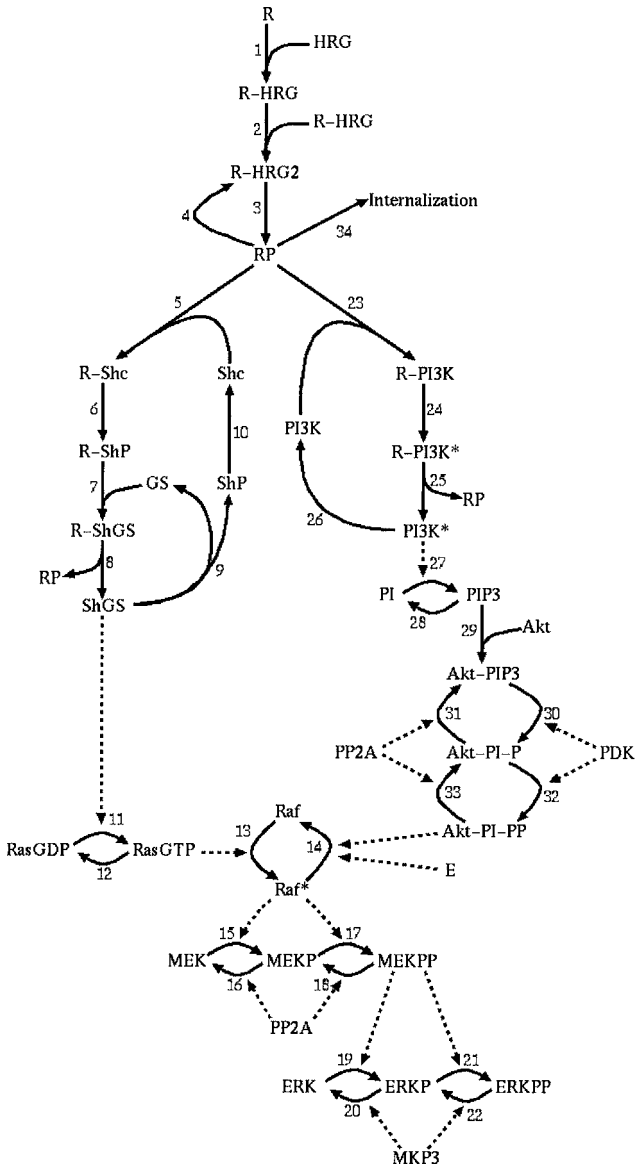

Scheme 1 Kinetic model of HRG-induced ErbB4 receptor signalling cascade

HRG-bound ErbB4 receptor initiates the Shc-Ras-Raf-MEK-ERK and PI-3K-Akt pathways. The active form of Akt negatively regulates the activation of Raf-1. ——, mass action; - - - -, Michaelis–Menten kinetics. The indicated numbers correspond to the kinetic equations in Tables 2 and 3.

binding sites for the phosphotyrosine-binding (PTB) domain of Shc and for the SH2 domain of p85 [27]. The binding kinetics of these two molecules to the receptor was assumed to be competitive [22].

For Shc signalling, we adopted the models and kinetic parameters from the EGFR simulation model described in [4,5,28,29], with some slight modifications. Shc was assumed to bind to Grb2–Sos complex (GS) in the model, since an earlier surface plasmon resonance experiment showed that tyrosine-phosphorylated Shc peptide (pY317) had a much higher affinity to GS than a single Grb2 molecule [30]. Guanine nucleotide exchange factor Sos accelerates GDP–GTP exchange on Ras protein, and Ras GTPase-activating protein (GAP) accelerates turnover of GTP hydrolysis by 10 000-fold when GAP is associated with RasGTP [31]. Therefore reaction 11 was taken

Table 1 Kinetic parameters for the HRG-induced ErbB4 signalling model

Known parameters were taken from the literature [4,5, 29,44–46], and the unknown parameters were estimated by the estimator using genetic algorithm. Michaelis–Menten constants (K_4, $K_{10}-K_{22}$, $K_{26}-K_{28}$, $K_{30}-K_{33}$) are given in nM. V_4, V_{10}, V_{12}, V_{26}, V_{28}, V_{30} and V_{32} are expressed in $nM \cdot s^{-1}$. First- and second-order rate constants are given in s^{-1} and $nM^{-1} \cdot s^{-1}$ respectively.

Parameter value	Reference	Parameter value	Reference
$k_1 = 1.2 \times 10^{-3}$	[44]	$k_{-1} = 7.6 \times 10^{-4}$	[44]
$k_2 = 0.01$	[5]	$k_{-2} = 0.1$	[5]
$k_3 = 1.0$	[5]	$k_{-3} = 0.01$	[5]
$V_4 = 62.5$	Estimation	$K_4 = 50$	[5]
$k_5 = 0.1$	[29]	$k_{-5} = 1$	[29]
$k_6 = 20$	[29]	$k_{-6} = 5$	[29]
$k_7 = 60$	Estimation	$k_{-7} = 546$	Estimation
$k_8 = 2040$	Estimation	$k_{-8} = 15700$	Estimation
$k_9 = 40.8$	Estimation	$k_{-9} = 0$	Estimation
$V_{10} = 0.0154$	Estimation	$K_{10} = 340$	[5]
$k_{11} = 0.222$	Estimation	$K_{11} = 0.181$	Estimation
$V_{12} = 0.289$	Estimation	$K_{12} = 0.0571$	Estimation
$k_{13} = 1.53$	Estimation	$K_{13} = 11.7$	Estimation
$k_{14} = 6.73 \times 10^{-3}$	Estimation	$K_{14} = 8.07$	Estimation
$k_{15} = 3.5$	Estimation	$K_{15} = 317$	[4]
$k_{16} = 0.058$	[4]	$K_{16} = 2200$	[4]
$k_{17} = 2.9$	[4]	$K_{17} = 317$	[4]
$k_{18} = 0.058$	[4]	$K_{18} = 60$	[4]
$k_{19} = 9.5$	[4]	$K_{19} = 1.46 \times 10^5$	[4]
$k_{20} = 0.3$	[4]	$K_{20} = 160$	[4]
$k_{21} = 16$	Estimation	$K_{21} = 1.46 \times 10^5$	[4]
$k_{22} = 0.27$	[4]	$K_{22} = 60$	[4]
$k_{23} = 0.1$	[29]	$k_{-23} = 2$	[29]
$k_{24} = 9.85$	[29]	$k_{-24} = 0.0985$	[29]
$k_{25} = 45.8$	[29]	$k_{-25} = 0.047$	[29]
$V_{26} = 2620$	Estimation	$K_{26} = 3680$	Estimation
$k_{27} = 16.9$	Estimation	$K_{27} = 39.1$	Estimation
$V_{28} = 17000$	Estimation	$K_{28} = 9.02$	Estimation
$k_{29} = 507$	Estimation	$K_{29} = 234$	Estimation
$V_{30} = k_{30}[\text{PDK}] = 2 \times 10^4$	[45]	$K_{30} = 80000$	[45]
$k_{31} = 0.107$	Estimation	$K_{31} = 4.35$	Estimation
$V_{32} = k_{32}[\text{PDK}] = 2 \times 10^4$	[45]	$K_{32} = 80000$	[45]
$k_{33} = 0.211$	Estimation	$K_{33} = 12$	Estimation
$k_{34} = 1 \times 10^{-3}$	[46]	$k_{-34} = 0$	[46]

from Brightman and Fell [6] and expressed as follows:

$$\text{RasGDP} + \text{ShGS} + \text{Pi} \Leftrightarrow \text{RasGDP} - \text{ShGS} + \text{Pi} \rightarrow \text{RasGTP} + \text{ShGS} \quad (1)$$

$$\text{RasGTP} + \text{GAP} \Leftrightarrow \text{RasGTP} - \text{GAP} \rightarrow \text{RasGDP} + \text{GAP} + \text{Pi}$$

where Pi represents a phosphate.

The activation and regulation of Raf-1 kinase are complex. Although the mechanism of Raf-1 kinase activation remains unclear, recent studies [17,32] have shown that the phosphorylation of Ser^{259} on Raf-1 serves as a regulatory switch for this activation. When Raf-1 on Ser^{259} is phosphorylated, Raf-1 (an unactivated form) is translocated to the cell membrane and binds to RasGTP. This binding step is a critical step for Raf-1 activation. The next three steps after this binding are dephosphorylation of Raf on Ser^{259} [Raf^* (an activated form of Raf)], activation of Raf-1 and activation of MEK. Finally, Raf-1 on Ser^{259} is rephosphorylated by an unknown kinase (enzyme 'E') in a Ras-dependent manner to attenuate the signal.

The mechanism of Raf-1 activation is described in the following approximation:

$$\text{RasGTP} + \text{Raf} \Leftrightarrow \text{RasGTP} - \text{Raf} \rightarrow \text{RasGTP} + \text{Raf}^* + \text{Pi} \quad (2)$$

$$\text{Raf}^* + \text{E} + \text{Pi} \Leftrightarrow \text{Raf}^* - \text{E} - \text{Pi} \rightarrow \text{Raf} + \text{E}$$

Table 2 Rate equations for HRG-induced ErbB4 signalling

Akt-PI-P, a PIP_3-bound singly phosphorylated form of Akt; Akt-PI-PP, a PIP_3-bound doubly phosphorylated form of Akt; ERKP, a singly phosphorylated form of ERK; MEKP, a singly phosphorylated form of MEK; R, an ErbB4 receptor; RP, a phosphorylated form of ErbB4 receptor.

Reaction number	Rate equation
1	$k_1[\text{R}][\text{HRG}] - k_{-1}[\text{R-HRG}]$
2	$k_2[\text{R-HRG}]^2 - k_{-2}[\text{R-HRG2}]$
3	$k_3[\text{R-HRG2}] - k_{-3}[\text{RP}]$
4	$V_4[\text{RP}]/(K_4 + [\text{RP}])$
5	$k_5[\text{RP}][\text{Shc}] - k_{-5}[\text{R-Shc}]$
6	$k_6[\text{R-Shc}] - k_{-6}[\text{R-ShP}]$
7	$k_7[\text{R-ShP}][\text{GS}] - k_{-7}[\text{R-ShGS}]$
8	$k_8[\text{R-ShGS}] - k_{-8}[\text{ShGS}][\text{RP}]$
9	$k_9[\text{ShGS}] - k_{-9}[\text{GS}][\text{ShP}]$
10	$V_{10}[\text{ShP}]/(K_{10} + [\text{ShP}])$
11	$k_{11}[\text{ShGS}][\text{RasGDP}]/(K_{11} + [\text{RasGDP}])$
12	$V_{12}[\text{RasGTP}]/(K_{12} + [\text{RasGTP}])$
13	$k_{13}[\text{RasGTP}][\text{Raf}]/(K_{13} + [\text{Raf}])$
14	$k_{14}([\text{Akt-PI-PP}] + [\text{E}])[\text{Raf}^*]/(K_{14} + [\text{Raf}^*])$
15	$k_{15}[\text{Raf}^*][\text{MEK}] \Big/ \left[K_{15}\left(1 + \frac{[\text{MEKP}]}{K_{17}}\right) + [\text{MEK}]\right]$
16	$k_{16}[\text{PP2A}][\text{MEKP}] \Big/ \left[K_{16}\left(1 + \frac{[\text{MEKP}]}{K_{18}} + \frac{[\text{Akt-PI-P}]}{K_{31}} + \frac{[\text{Akt-PI-PP}]}{K_{33}}\right) + [\text{MEKP}]\right]$
17	$k_{17}[\text{Raf}^*][\text{MEKP}] \left[K_{17}\left(1 + \frac{[\text{MEK}]}{K_{15}}\right) + [\text{MEKP}]\right]$
18	$k_{18}[\text{PP2A}][\text{MEKPP}] \Big/ \left[K_{18}\left(1 + \frac{[\text{MEKP}]}{K_{16}} + \frac{[\text{Akt-PI-P}]}{K_{31}} + \frac{[\text{Akt-PI-PP}]}{K_{33}}\right) + [\text{MEKPP}]\right]$
19	$k_{19}[\text{MEKPP}][\text{ERK}] \Big/ \left[K_{19}\left(1 + \frac{[\text{ERKP}]}{K_{21}}\right) + [\text{ERK}]\right]$
20	$k_{20}[\text{MKP3}][\text{ERKP}] \Big/ \left[K_{20}\left(1 + \frac{[\text{ERKPP}]}{K_{22}}\right) + [\text{ERKP}]\right]$
21	$k_{21}[\text{MEKPP}][\text{ERKP}] \Big/ \left[K_{21}\left(1 + \frac{[\text{ERK}]}{K_{19}}\right) + [\text{ERKP}]\right]$
22	$k_{22}[\text{MKP3}][\text{ERKPP}] \Big/ \left[K_{22}\left(1 + \frac{[\text{ERKP}]}{K_{20}}\right) + [\text{ERKPP}]\right]$
23	$k_{23}[\text{RP}][\text{PI3K}] - k_{-23}[\text{R-PI-3K}]$
24	$k_{24}[\text{R-PI3K}] - k_{-24}[\text{R-PI-3K}^*]$
25	$k_{25}[\text{R-PI3K}^*] - k_{-25}[\text{RP}][\text{PI-3K}^*]$
26	$V_{26}[\text{PI3K}^*]/(K_{26} + [\text{PI-3K}^*])$
27	$k_{27}[\text{PI3K}^*][\text{PI}]/(K_{27} + [\text{PI}])$
28	$V_{28}[\text{PIP}_3]/(K_{28} + [\text{PIP}_3])$
29	$k_{29}[\text{PIP}_3][\text{Akt}] - k_{-29}[\text{Akt-PIP}_3]$
30	$V_{30}[\text{Akt-PIP}_3] \Big/ \left[K_{30}\left(1 + \frac{[\text{Akt-PI-P}]}{K_{32}}\right) + [\text{Akt-PIP}_3]\right]$
31	$k_{31}[\text{PP2A}][\text{Akt-PI-P}] \Big/ \left[K_{31}\left(1 + \frac{[\text{MEKP}]}{K_{16}} + \frac{[\text{MEKPP}]}{K_{18}} + \frac{[\text{Akt-PI-PP}]}{K_{33}}\right) + [\text{Akt-PI-P}]\right]$
32	$V_{32}[\text{Akt-PI-P}] \Big/ \left[K_{32}\left(1 + \frac{[\text{Akt-PIP}_3]}{K_{30}}\right) + [\text{Akt-PI-P}]\right]$
33	$k_{33}[\text{PP2A}][\text{Akt-PI-PP}] \Big/ \left[K_{33}\left(1 + \frac{[\text{MEKP}]}{K_{16}} + \frac{[\text{MEKPP}]}{K_{18}} + \frac{[\text{Akt-PI-P}]}{K_{31}}\right) + [\text{Akt-PI-P}]\right]$
34	$k_{34}[\text{RP}] - k_{-34}[\text{internalization}]$

An activated form of Raf-1 catalyses the double phosphorylation of MEK on certain serine/threonine residues. Phosphorylated MEK (MEKPP) phosphorylates threonine/tyrosine residues of ERK. Phosphorylated ERK (ERKPP), in turn, activates transcription factors after its relocation to nuclei [33]. The MAPK cascade is negatively regulated by MAPK phosphatase 3 (MKP3) for the dephosphorylation of ERK and by PP2A for the dephosphorylation of MEK [34,35]. On the other hand, PI3K activation in HRG-stimulated cells was confirmed to cause Akt activation in our experiment. The mechanism of PI3K-initiated Akt activation can be explained as follows: PI3K catalyses the phosphorylation of phosphatidylinositol (PI) on the inner surface of the cell membrane and generates phosphatidylinositol-3,4-biphosphate (PIP_2) and phosphatidylinositol-3,4,5-trisphosphate (PIP_3). PIP_3 binds to the pleckstrin homology (PH) domain of Akt and translocates the enzyme to the inner surface of the

Table 3 Kinetic equations for the model

The numbers of the rate constants correspond to the reaction numbers in Table 2.

Equation
$d[Akt]/dt = -v_{29}$
$d[Akt\text{-}PIP_3]/dt = v_{29} - v_{30} + v_{31}$
$d[Akt\text{-}PI\text{-}P]/dt = v_{30} - v_{31} - v_{32} + v_{33}$
$d[Akt\text{-}PI\text{-}PP]/dt = v_{32} - v_{33}$
$d[ERK]/dt = -v_{19} + v_{20}$
$d[ERKP]/dt = v_{19} - v_{20} - v_{21} + v_{22}$
$d[ERKPP]/dt = v_{21} - v_{22}$
$d[GS]/dt = -v_7 + v_9$
$d[HRG]/dt = -v_1$
$d[internalization]/dt = v_{34}$
$d[MEK]/dt = -v_{15} + v_{16}$
$d[MEKP]/dt = v_{15} - v_{16} - v_{17} + v_{18}$
$d[MEKPP]/dt = v_{17} - v_{18}$
$d[PI]/dt = -v_{27} + v_{28}$
$d[PI3K]/dt = -v_{23} + v_{26}$
$d[PI3K^*]/dt = v_{25} - v_{26}$
$d[PIP_3]/dt = v_{27} - v_{28} - v_{29}$
$d[R]/dt = -v_1$
$d[RP]/dt = v_3 - v_4 - v_5 + v_8 - v_{23} + v_{25} - v_{34}$
$d[R\text{-}HRG]/dt = v_1 - 2v_2$
$d[R\text{-}HRG2]/dt = v_2 - v_3 + v_4$
$d[R\text{-}PI3K]/dt = v_{23} - v_{24}$
$d[R\text{-}PI3K^*]/dt = v_{24} - v_{25}$
$d[R\text{-}ShGS]/dt = v_7 - v_8$
$d[R\text{-}ShP]/dt = v_6 - v_7$
$d[R\text{-}Shc]/dt = v_5 - v_6$
$d[Raf]/dt = -v_{13} + v_{14}$
$d[Raf^*]/dt = v_{13} - v_{14}$
$d[RasGDP]/dt = -v_{11} + v_{12}$
$d[RasGTP]/dt = v_{11} - v_{12}$
$d[ShGS]/dt = v_8 - v_9$
$d[ShP]/dt = v_9 - v_{10}$
$d[Shc]/dt = -v_5 + v_{10}$

plasma membrane before the activation [15,36]. Akt is regulated by 3′-phosphoinositide-dependent protein kinase 1 (PDK1) on Thr^{308} and Ser^{473} [37,38]. This double phosphorylation is essential for the full activation of Akt [Akt-PI-PP (a PIP_3-bound doubly phosphorylated form of Akt)], but the Ser^{473} phosphorylation plays a far more important role than the Thr^{308} phosphorylation, accounting for more than 90% of the enzymic activity of Akt [24]. Whereas PDK1 has the PH domain and associates with the basal level of PIP_3 with a much higher affinity than Akt, PDK1 is a constitutively active enzyme that generally maintains the same activity and localization for Akt phosphorylation when exposed to growth factor stimulation [39]. Dephosphorylation by PP2A attenuates the activation of Akt [40,41]. Alternatively, PIP_3 is dephosphorylated by phosphatase and tensin homologues (PTEN) and thereby turns the signal off [42,43].

As experimentally demonstrated in ErbB4-expressing cells, Raf-1 is additionally inactivated by Akt in a PI-3K-dependent manner through Ser^{259} phosphorylation. In short, phosphorylation of Raf-1 on Ser^{259} was doubly regulated by an unknown kinase (enzyme 'E') in a Ras-dependent manner and by Akt in a PI-3K-dependent manner [17,18]. We modelled this cross-talk between Akt and Raf-1 in HRG-induced ErbB4 receptor signalling.

Tables 1–4 summarize the kinetic parameters and ordinary differential equations used for the simulation. Known rate constants were taken from the literature listed, and unavailable kinetic parameters were estimated using the parameter estimator. Cellular protein concentrations were estimated over the range of 1–1000 nM [5,29,44–46].

Table 4 Initial concentrations of the cellular components

Reactant	Concentration (nM)
ErbB4 receptor (R)	80
Shc	1000
Grb2-Sos (GS)	10
RasGDP	120
Raf-1	100
MEK	120
ERK	1000
PI3K	10
PI	800
Akt	10
Enzyme 'E'	7
MKP3	2.4
PP2A	11.4

Our model employs the Michaelis–Menten approximation for most of the enzymic reactions (PI3K, Raf*, MEKPP, ERKPP, Akt-PI-PP and enzyme 'E') and the interaction of Shc-GS (ShGS) with RasGDP. The following reaction sets in Scheme 1 share common enzymes individually: reactions 15 and 17 for activated Raf-1, reactions 16, 18, 31 and 33 for PP2A, reactions 19 and 21 for activated MEK, reactions 20 and 22 for MKP3 and reactions 30 and 32 for PDK1. The concentrations of the active enzymes in reactions 11, 13–15, 17, 19, 21 and 27 in Scheme 1 were assumed not to remain constant throughout the reactions. We used the formula by Kholodenko [29] to express the conversions of the active and inactive enzymes. To express the production rates for the enzymic reactions (e.g. reactions 16, 18, 31 and 33) that recruit a common enzyme (e.g. PP2A), we used the equations presented in Appendix B. Regarding the turnover of ErbB4 receptor after ligand binding, the rate of internalization and degradation of ErbB4 is slower than that of EGFR, or is approx. 0.001 s^{-1} according to our calculation [47].

Simulation on HRG-induced ErbB4 signalling

When the simulation model was used to examine HRG (10 nM), the result showed the following: transient receptor phosphorylation reached a peak within 1 min, MEK and ERK activation from 5 to 10 min, rapid activation of Akt activity within 2 min and sustained Akt activity over the entire time course (Figures 4A–4G). When lower concentrations of HRG (0.1–10 nM) were added, receptor phosphorylation, Akt, MEK and ERK phosphorylation levels also varied in a dose-dependent manner. These results are consistent with our experimental results.

We monitored the reaction rates of phosphorylation and dephosphorylation reactions (reactions 11–22 and 27–33 in Scheme 1) during the simulation period to understand the dynamics of the kinases and phosphatases on the signal amplitude in each step (Figure 5). In these Figures, kinases in the MAPK cascade generally showed a higher reaction rate than the corresponding phosphatases at early time points where amplification of the signals is observed; the reaction rate of the phosphatases slowly increased and retained a higher rate than the kinases at later time points (Figures 5B–5F). In contrast, phosphorylation and dephosphorylation reactions of Ras GDP–GTP exchange (Figure 5A) and PI (Figure 5G) showed almost identical reaction rates in forward and backward reactions, indicating that turnover of the activated form of the reactants is rapid. Since Ras GDP–GTP exchange is a limiting step for the MAPK cascade, this GDP–GTP exchange balance to induce rapid GTP hydrolysis seemed to be biologically relevant [47]. Overall, the time course

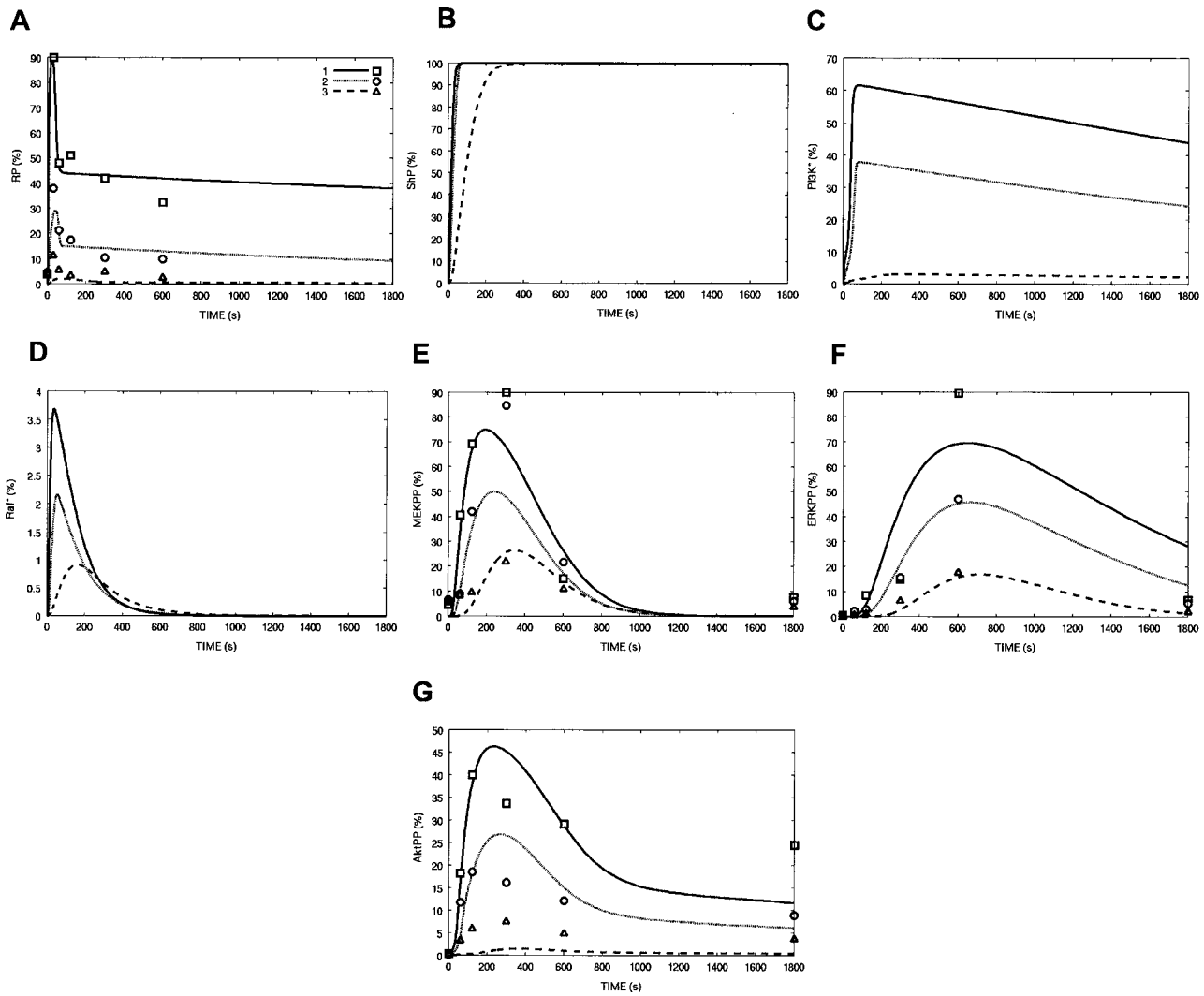

Figure 4 Computer simulation of HRG-induced ErbB4 signalling cascade at different HRG concentrations

(**A**) Phosphorylation of the ErbB4 receptor (RP); (**B**) phosphorylation of Shc (ShP); (**C**) activation of PI3K (PI3K*); (**D**) activation of Raf-1 (Raf*); (**E**) activation of MEK (MEKPP); (**F**) activation of ERK (ERKPP); (**G**) activation of Akt (Akt-PI-PP). In (**A**, **E**–**G**), symbols show experimental results of Western-blot analysis (——, □, 10 nM;, – – –, ○, 1 nM; · · · · · · · · ·, △, 0.1 nM).

of the reaction rates in phosphorylation reactions, rather than dephosphorylation reactions, well reflected the patterns of the signal amplitude.

Effect of PI-3K inhibitor

Next, we simulated the effect of PI3K inhibition on the kinetics of ERK and Akt activation. Since wortmannin is an irreversible inhibitor of PI3K [48] and functionally lowers the V_{max} of this enzyme, we set a lower V_{max} value for the enzymic activity of PI3K (Figure 6).

As a result, a lower V_{max} for enzymic activity of PI3K caused a higher activation in ERK. On the other hand, Akt activity was decreased under the same condition, dwindling almost to nothing when the V_{max} was set at 1/100th of the initial value. This simulation well reflected a pattern similar to that of the experimental result (Figure 2B).

PP2A regulates the activities of MEK and Akt

Since PP2A deactivates both MEK and Akt within a short time period, sharing of the common enzyme PP2A with either of the active forms of MEK and Akt may affect the downstream kinetics of ERK activity. We examined whether such an availability of PP2A and Raf-Akt cross-talk is a truly major regulatory mechanism for ERK activity in HRG signalling. We compared the simulation results obtained from the following three models: (A) with the sharing of PP2A and Raf-Akt cross-talk (the original model); (B) without the sharing of PP2A (the activated forms of MEK and Akt do not share the same enzyme; reactions 16 and 18 differ from reactions 31 and 33); (C) without Raf-Akt cross-talk (the activated form of Akt does not stimulate reaction 14). In this test, the initial concentration of Akt was set four times higher than the original concentration (40 nM) to derive a significant difference in each ERK activity in the presence or absence of wortmannin (V_{max} = 1/100 of the original value). In conclusion, the three models showed characteristically different patterns of ERK activity. The results observed in the model with both sharing of PP2A with the active forms of MEK and Akt and Raf-Akt cross-talk (i.e. an earlier and higher peak in ERK in the presence of wortmannin; Figure 7A) were the most consistent with the results experimentally observed in our laboratory (Figure 2B), as well as with the results observed in IGF-1-stimulated MCF-7

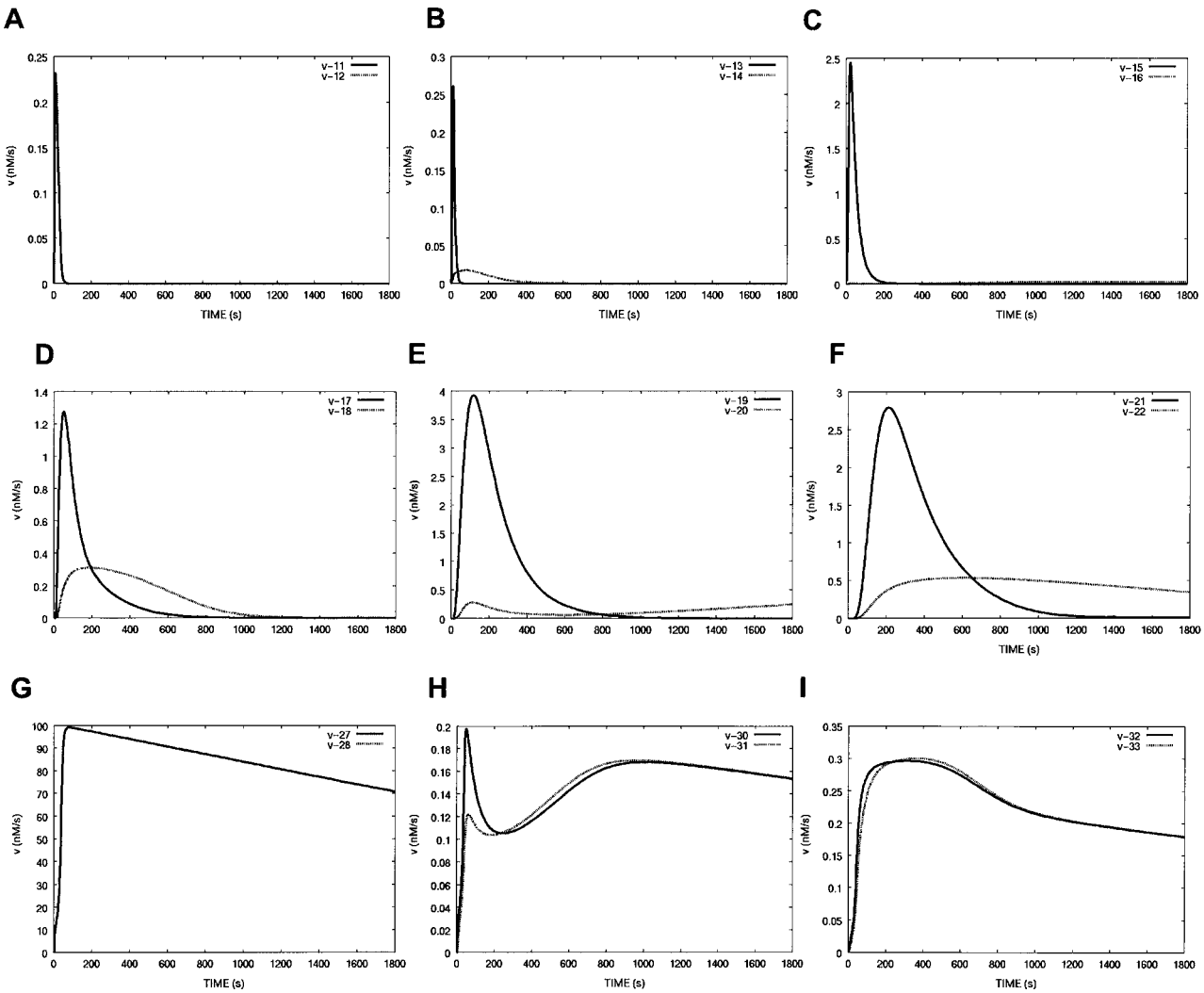

Figure 5 Reaction rates of kinase and phosphatase

(**A**) Ras GDP–GTP exchange, reactions 11 and 12 in Scheme 1; (**B**) Raf → Raf* conversion, reactions 13 and 14; (**C**) MEK phosphorylation and MEKP dephosphorylation, reactions 15 and 16; (**D**) MEKP phosphorylation and MEKPP dephosphorylation; reactions 17 and 18; (**E**) ERK phosphorylation and ERKP dephosphorylation, reactions 19 and 20; (**F**) ERKP phosphorylation and ERKPP dephosphorylation, reactions 21 and 22; (**G**) PI phosphorylation and dephosphorylation, reactions 27 and 28; (**H**) Akt-PIP_3 phosphorylation and Akt-PI-P (a PIP_3-bound singly phosphorylated form of Akt) dephosphorylation, reactions 30 and 31; (**I**) Akt-PI-P phosphorylation and Akt-PI-PP dephosphorylation, reactions 32 and 33. ——, kinases; · · · · · · · · ·, phosphatases.

cells, a cell line that also possesses Raf-Akt cross-talk [18]. On the other hand, in the model without sharing of PP2A, wortmannin elicited a later and higher peak of ERK activity (Figure 7B), and without Raf-Akt cross-talk, wortmannin elicited early but inhibited ERK activity (Figure 7C). Although these simulation results may only be hypothetical for real cellular events, we find it significant that our simulation model reflected the experimental results only under the condition where both Raf-Akt cross-talk and sharing of PP2A were present. Given this finding, it seems highly likely that this dual regulation is responsible for the kinetic regulation of ERK activity.

Since PP2A is recruited to both MEK and Akt pathways, the total amount of PP2A and the affinity of PP2A to the active forms of MEK and Akt also affects the downstream kinetics of ERK and Akt activities. In our simulation model, V_{max} and K_m in the corresponding reactions reflect the concentration and affinities of PP2A to MEK and Akt respectively. To illustrate the kinetic character of PP2A on MEK and Akt, we set the K_m for reactions 16 and 18 (MEK dephosphorylation) as equal, and for reactions 31 and 33 (Akt dephosphorylation) as equal. Similarly, we set the V_{max} for the above reactions as equal: $V_{max} = 0.058$[PP2A] and $K_m = \alpha K_{MEK}$ for reactions 16 and 18, and $V_{max} = 0.1747$[PP2A] and $K_m = \alpha K_{Akt}$ for reactions 31 and 33, where α is a multiplicative factor. The affinity ratio β is expressed as $\beta = K_{MEK}/K_{Akt}$. These parameters (α, β and PP2A concentration) were varied to monitor the effect of concentration and the affinities of PP2A on downstream ERK and Akt activities (Figure 8). As a result, the activities of ERK and Akt are suppressed in a PP2A-concentration-dependent manner and a high concentration of PP2A eliminated all ERK and Akt activities where $\alpha = 1$ or 10 (Figures 8A–8D). The graphs also showed that a higher affinity of PP2A to MEK (β is small) decreased ERK activation and increased Akt activation (Figures 8A–8F). Where β is large, ERK shows high activity. Akt shows low activity where PP2A concentration is high (Figures 8C and 8D). This mechanism underlies the sharing of the common enzyme PP2A in our

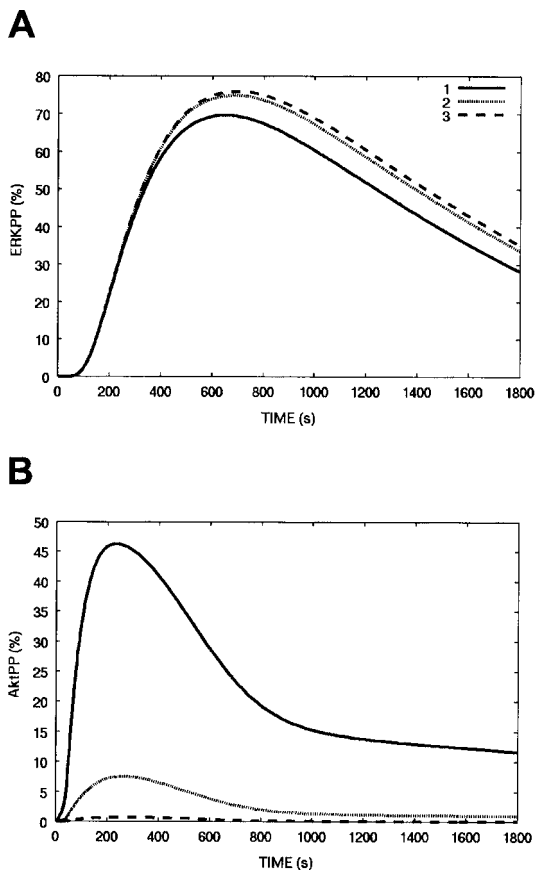

Figure 6 Effect of the PI3K inhibitor wortmannin on ERK and Akt activation

Wortmannin is an irreversible inhibitor and lowers the V_{max} of PI-3K. Line 1, original V_{max}; line 2, 1/10; line 3, 1/100.

simulation model. The affinity ratio β seemed to be crucial especially when α is 1–10^2. Since the K_m value represents the affinity of an enzyme (in this case, PP2A) for a substrate (MEK or Akt) and implies catalytic activity of the enzyme towards the substrate, a larger K_m value means lower enzyme activity. When the K_m value is large enough for a PP2A reaction, the effect of PP2A concentration is only negligible, and apparent kinase activities reach a 100 % maximum. In our model, when α is approx. 10^4, both ERK and Akt gained maximal enzymic activity independent of β and there appeared to be no Raf-Akt cross-talk or regulatory effect of PP2A concentration (Figures 8I and 8J). This is because MEK and Akt cascades have no reverse reactions to reduce the active forms of the enzymes, meaning that in practical terms this model can behave as two different signalling models, depending on the kinetic parameter of the kinases and phosphatases. In particular, it may be assumed that the kinetic parameters of PP2A significantly affect downstream kinase activities.

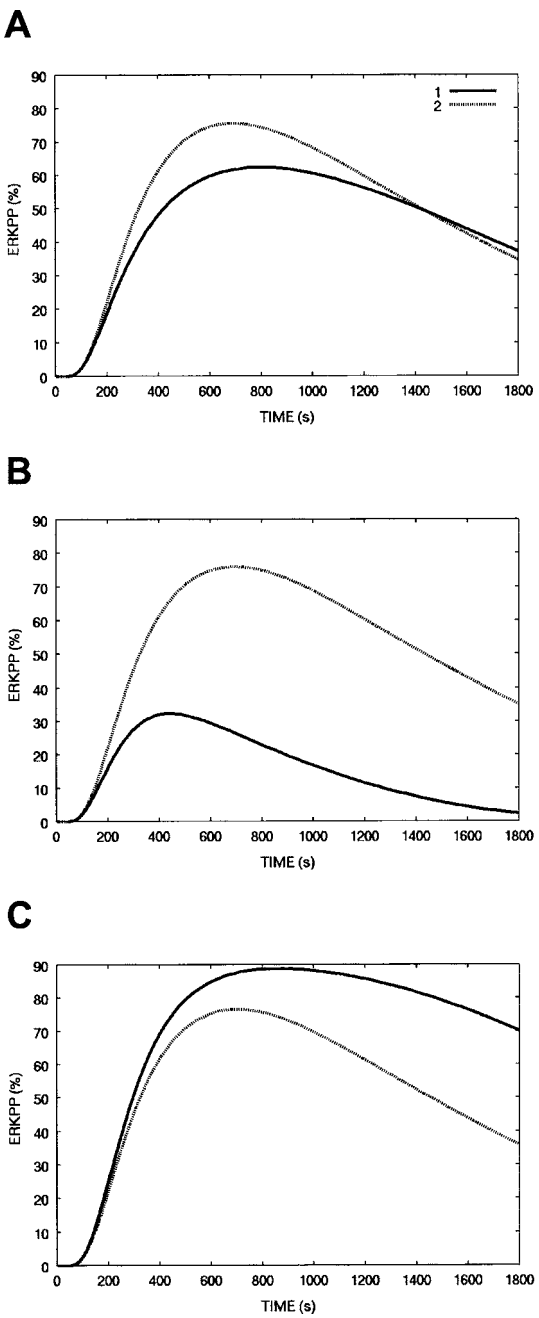

Figure 7 Evaluation of the models with or without PP2A competition and Raf-Akt cross-talk

The initial concentration of Akt was set at 40 nM. The solid line shows the ERK activity of the cells treated with HRG and the dotted line shows the cells treated with wortmannin and HRG. (**A**) Both PP2A competition and Raf-Akt cross-talk exist (the original model). (**B**) There is no competition of PP2A (MEKPP and Akt-PI-PP do not share the same enzyme). (**C**) There is no Raf-Akt cross-talk (Akt-PI-PP does not convert Raf* → Raf).

DISCUSSION

There is increasing evidence that PI3K, largely responsible for cell survival and differentiation, interferes with ERK activity [49–51]. In addition to demonstrating Akt-induced suppression of ERK in growth-hormone-induced signalling pathways in several cell lines, our experiments in the present study confirmed that a similar mode of ERK inhibition took place in HRG-induced ErbB4 signalling in ErbB4-expressing CHO cells. We formulated these experimental observations in a mathematical model to understand the complex mechanisms of kinase regulation in cellular signalling cascade. Overall, our mathematical model accurately reflected the experimental data and yielded clues to understand the regulatory mechanism of Raf-Akt cross-talk. In our evaluation of the model, we found that it encompassed major

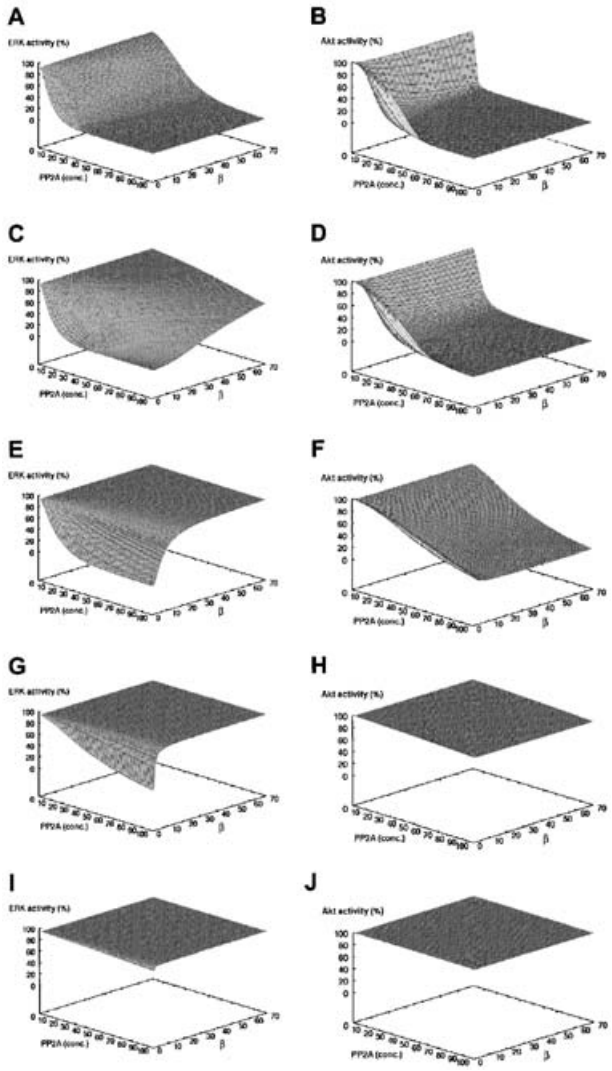

Figure 8 Effect of the affinity and concentration of PP2A on ERK and Akt activities

The K_m values for reactions 16 and 18 in Scheme 1 (MEK dephosphorylation) were set as equal and the K_m values for reactions 31 and 33 (Akt dephosphorylation) were set as equal; $V_{max} = 0.058$[PP2A], $K_m = \alpha K_{MEK}$ for reactions 16 and 18 were set as equal; $V_{max} = 0.1747$[PP2A], $K_m = \alpha K_{Akt}$ for reactions 31 and 33, and were set as equal; α is a multiplicative factor. The affinity ratio β is expressed as $\beta = K_{MEK}/K_{Akt}$. α, β and PP2A concentration was varied to monitor ERK and Akt activities. ERK and Akt activities (%) were expressed as a ratio showing the active form of the kinases in the total concentration of the kinases. PP2A concentration is expressed in nM. (**A**) and (**B**), $\alpha = 1$; (**C**) and (**D**), $\alpha = 10$; (**E**) and (**G**), $\alpha = 10^2$; (**F**) and (**H**), $\alpha = 10^3$; (**I**) and (**J**), $\alpha = 10^4$. (**A**), (**C**), (**E**), (**G**) and (**I**) show ERK activities, and (**B**), (**D**), (**F**), (**H**) and (**J**) show Akt activities.

regulatory systems to modulate ERK activity. One is the cross-talk between Raf-MEK-ERK and PI-3K-Akt pathways, and the other is the regulation by PP2A.

In the course of our analysis, we found that our model behaved as two different signalling models, either possessing or not possessing Raf-Akt cross-talk, depending on the kinetic parameters of PP2A. A similar phenomenon is observed in IGF-1-activated signalling pathways, where high doses of IGF-1 triggered Raf-Akt cross-talk but low doses of IGF-1 did not [18]. Similarly, it has been reported that platelet-derived growth factor receptor-induced long-sustained Akt activity results in Raf-Akt cross-talk, but protease-activated receptor-induced weak Akt activity did not have a similar effect in vascular smooth-muscle cells [22]. In our model, sustained Akt activity can be reproduced where a weak association between Akt and PP2A and a strong association between MEK and PP2A co-exist, and this condition inhibits ERK activity. In contrast, opposite conditions do not cause ERK inhibition. When the catalytic activity of PP2A is very low for ERK and Akt reactions, there is no apparent Raf-Akt cross-talk. As was the case in an earlier study by Heinrich et al. [52], our model containing cross-talk showed drastic changes in dynamic behaviour in response to small parameter variation. If no qualitative difference occurs in the signal transduction of the above IGF-1 signalling pathways, regulation of phosphatase activity will affect quite probably the kinetics of Akt and ERK activities. Localization mechanisms of PP2A in the reaction sites, structural change or modification of the corresponding proteins to influence the affinity and the catalytic activity of PP2A may possibly induce such phenomena in cells.

Despite the fact that PP2A is an abundant phosphatase and is supposed to exist at the micromolar range in the cells [53], we estimated the concentration to be as low as 11 nM. In our model, when the concentration is as high as 100 nM, PP2A totally suppresses ERK and Akt activities. Considering that PP2A contributes to a wide variety of cellular events such as DNA replication and transcription, RNA splicing, translation, cell-cycle progression, morphogenesis and the regulation of a variety of signal transduction cascades [54,55], its localization and availability rather than the absolute amount of PP2A appear to affect temporal signalling dynamics. Moreover, PP2A activity is tightly regulated by the use of different subunits and its expression is highly controlled [55]. The apparent PP2A concentration available for specific cellular phenomena may be much lower than the physiologically known concentration. A similar explanation may apply to PI3K and Akt, the concentration of which is much lower than that of other signalling reactants, and these kinases should have other roles to play in cellular differentiation cascade or prevention of apoptosis rather than in Raf inhibition.

There is increasing evidence that the amplification mechanism of signal transduction cascade is regulated by phosphatases as well as kinases, and a computer simulation approach applying the kinetic model is quite useful to evaluate this type of regulatory mechanism. PP2A is a serine/threonine phosphatase that plays a central role in the regulation of protein kinases that are transiently phosphorylated and activated, and PP2A appears to determine the activation kinetics of a protein kinase cascade [18,40,41,56,57]. Although our model focused on the deactivation of Akt and MEK by PP2A, the Raf-1 protein is known to be positively regulated by the same enzyme [17]. As Raf-1 serves as the heart of several signalling networks, this regulation mechanism is complicated and remains largely unknown. Nonetheless, given that the Raf-1 translocation to the membrane and its binding with Ras are limiting steps for Raf-1 activation, we can safely affirm that the dephosphorylation of Raf-1 by PP2A is not a kinetic limiting factor for Raf-1 activation [17].

It is known that PI3K begins bestowing positive effects on ERK later during growth hormone signalling (after approx. 30 min), probably through Rac or PAK [18,58]. In HRG-stimulated cells, Gab2 is reported to regulate negatively Ras-PI3K activation via negative feedback through the PI3K-Akt pathway [59]. It has been recently found that PI3K and its enzymic products have many regulatory roles in membrane receptor-mediated signal transduction cascade. Whereas PI3K binds directly to the receptor molecule in our model, PI3K binds to the receptor via Gab1 and positively regulates ERK in EGFR signalling. The PI3K product PIP_3 also induces up-regulation of ERK by additionally recruiting Gab1 to the activated receptor

[50]. Given the complexity of the regulatory mechanism of PI3K, a regulatory model of this type involving PI3K might facilitate our understanding of the cellular behaviour more accurately.

One of the challenging purposes of ErbB modelling was to resolve unknown mechanisms causing malignant phenotypes when different ErbB receptors were co-expressed in the same cells. For example, long-term treatment of ErbBs-co-expressing cells with growth factor induced cellular transformation, whereas a single ErbB receptor triggered no such effect [60,61]. An ensemble of qualitative experimental data may not be sufficient to resolve these unknown mechanisms. As an alternative, we propose that a mathematical quantitative analysis of the signal transduction cascade will provide a theoretical understanding of ErbB signalling that may prove useful to unravel the amplification mechanisms of the cellular phenomena caused by ErbB receptors.

APPENDIX A

DIDC algorithm (a genetic algorithm with Distance Independent Diversity Control)

We used DIDC as a parameter estimator to obtain unknown kinetic constants and concentrations of cellular signalling molecules for our simulation model. DIDC is a real-coded genetic algorithm and was designed to solve high-dimensional and multi-modal function optimization problems. It uses two different search operators, ENDX (Extended Normal Distribution Crossover) and NDM (Normal Distribution Mutation).

The DIDC algorithm is as follows:

1. As an initial population, create n_p individuals randomly. Set Generation $= 0$ and a mutation applying probability of $p_m = 1$.
2. Go to step 3 with probability p_m. Otherwise, jump to step 4.
3. Select a pair of individuals randomly without replacing it from the population. Generate n_c children by applying NDM to the selected pair of individuals. Choose an individual with the best fitness from the family, which includes the parent. Exchange the parent for the selected individual. Jump to step 5.
4. Select a pair of individuals randomly without replacing it from the population. Generate n_c children by applying ENDX to the selected pair of individuals. Choose two individuals from the family. One has the best fitness, and the other is selected randomly. Exchange the parents for the selected individuals.
5. If the best individual in the population has not been improved in the last T_s generations, set the probability $p_m = 0$. Otherwise, set $p_m = 1$.
6. Generation $\leftarrow$ Generation $+$ 1. Return to step 2.

The parameters $T_s = 3n_p$, $n_p = 15n$ and $n_c = 50$ are recommended, where n is the dimension.

ENDX (Extended Normal Distribution Crossover) requires m parents.

Let randomly selected parental vectors be $\mathbf{p}_1, \ldots, \mathbf{p}_m$. ENDX generates a child vector $\mathbf{c}$ as follows: $\mathbf{c} = \mathbf{p} + \xi\mathbf{d} + \sum_{i=3}^{m} \eta_i \mathbf{p}'_i$, where $\mathbf{p} = (\mathbf{p}_1 + \mathbf{p}_2)/2$, $\mathbf{d} = \mathbf{p}_2 - \mathbf{p}_1$, $\mathbf{p}'_i = \mathbf{p}_i - [1/(m-2)] \sum_{j=3}^{m} \mathbf{p}_j$, $\xi \sim \mathrm{N}(0, \alpha^2)$, and $\eta_i \sim \mathrm{N}(0, \beta^2)$, $\alpha = 0.434$, $\beta = 0.35/\sqrt{m-3}$ and $m = n+2$ are recommended, and n is the dimension.

For the generation alternation, first, m parents are randomly selected, then ENDX generates n_c offspring using the m parents. Two individuals are selected from the family, which includes two parents ($\mathbf{p}_1$ and $\mathbf{p}_2$) and their offspring. One is the best individual. The other is selected randomly from the family. Finally, the two parents, $\mathbf{p}_1$ and $\mathbf{p}_2$, are exchanged for the selected offspring.

NDM (Normal Distribution Mutation) is very similar to ENDX.

Like ENDX, NDM uses m randomly selected parents. NDM generates a child vector $\mathbf{c}$ as follows: $\mathbf{c} = \mathbf{p}_i + \sum_{i=2}^{m} \eta_i \mathbf{p}''_i$, where $\mathbf{p}''_i = \mathbf{p}_i - [1/(m-1)] \sum_{j=2}^{m} \mathbf{p}_j$ and $\eta_i \sim \mathrm{N}(0, \gamma^2)$, and $\gamma = 0.35/\sqrt{m-2}$ and $m = n + 2$ are recommended.

For the generation alternation, m parents are randomly selected. NDM then also generates n_c offspring using the m parents. For the generation alternation, only one individual is selected (i.e. the best individual is selected from the family that includes the parent $\mathbf{p}_1$ and their offspring). Finally, the parent $\mathbf{p}_1$ is exchanged for the selected offspring.

APPENDIX B

Equations expressing the production rates for the two enzymic reactions that share the common enzyme PP2A

Let us consider two reactions of the simplest Michaelis–Menten type with a common enzyme 'E' that catalyses the conversion of substrates S_1 and S_2 into products P_1 and P_2 respectively as shown by the following equations:

$$S_1 + E \underset{k_{12}}{\overset{k_{11}}{\rightleftarrows}} S_1E \xrightarrow{k_{13}} P_1 + E$$

$$S_2 + E \underset{k_{22}}{\overset{k_{21}}{\rightleftarrows}} S_2E \xrightarrow{k_{23}} P_2 + E$$

The rate equations for the products and the enzyme–substrate complexes for each reaction are expressed as follows:

$$\frac{d[P_1]}{dt} = k_{13}[S_1E] \tag{B1}$$

$$\frac{d[P_2]}{dt} = k_{23}[S_2E] \tag{B2}$$

$$\frac{d[S_1E]}{dt} = k_{11}[S_1][E] - (k_{12} + k_{13})[S_1E] \tag{B3}$$

$$\frac{d[S_2E]}{dt} = k_{21}[S_2][E] - (k_{22} + k_{23})[S_2E] \tag{B4}$$

Assuming a quasi-steady-state approximation expressed as $d[S_1E]/dt = 0$ and $d[S_2E]/dt = 0$ for eqns (B3) and (B4), we have

$$[S_1E] = \frac{k_{11}[S_1][E]}{k_{12} + k_{13}} \tag{B5}$$

$$[S_2E] = \frac{k_{21}[S_2][E]}{k_{22} + k_{23}} \tag{B6}$$

Elimination of [E] in eqns (B5) and (B6) by means of the conservation law $[E]_0 = [E] + [S_1E] + [S_2E]$ yields the following equations:

$$\frac{d[P_1]}{dt} = \frac{V_1[S_1]}{K_1(1 + [S_1]/K_1 + [S_2]/K_2)} \tag{B7}$$

$$\frac{d[P_2]}{dt} = \frac{V_2[S_2]}{K_2(1 + [S_1]/K_1 + [S_2]/K_2)} \tag{B8}$$

where $V_1 = k_{13}[E]_0$, $K_1 = (k_{12} + k_{13})/k_{11}$, $V_2 = k_{23}[E]_0$ and $K_2 = (k_{22} + k_{23})/k_{21}$. Equations (B7) and (B8) express the production rates for the two enzymic reactions that share the common enzyme.

REFERENCES

1 Slamon, D. J., Clark, G. M., Wong, S. G., Levin, W. J., Ullrich, A. and McGuire, W. L. (1987) Human breast cancer: correlation of relapse and survival with amplification of the HER-2/neu oncogene. Science **235**, 177–182

2 Yarden, Y. and Sliwkowski, M. X. (2001) Untangling the ErbB signalling network. Nat. Rev. Mol. Cell. Biol. **2**, 127–137

3 Olayioye, M. A., Neve, R. M., Lane, H. A. and Hynes, N. E. (2000) The ErbB signaling network: receptor heterodimerization in development and cancer. EMBO J. **19**, 3159–3167

4 Schoeberl, B., Eichler-Jonsson, C., Gilles, E. D. and Müller, G. (2002) Computational modeling of the dynamics of the MAP kinase cascade activated by surface and internalized EGF receptors. Nat. Biotechnol. **20**, 370–375

5 Kholodenko, B. N., Demin, O. V., Moehren, G. and Hoek, J. B. (1999) Quantification of short term signaling by the epidermal growth factor receptor. J. Biol. Chem. **274**, 30169–30181

6 Brightman, F. A. and Fell, D. A. (2000) Differential feedback regulation of the MAPK cascade underlies the quantitative differences in EGF and NGF signalling in PC12 cells. FEBS Lett. **482**, 169–174

7 Bhalla, U. S. and Iyengar, R. (1999) Emergent properties of networks of biological signaling pathways. Science **283**, 381–387

8 Alroy, I. and Yarden, Y. (1997) The ErbB signaling network in embryogenesis and oncogenesis: signal diversification through combinatorial ligand–receptor interactions. FEBS Lett. **410**, 83–86

9 Riese, II, D. J., Kim, E. D., Elenius, K., Buckley, S., Klagsbrun, M., Plowman, G. D. and Stern, D. F. (1996) The epidermal growth factor receptor couples transforming growth factor-, heparin-binding epidermal growth factor-like factor, and amphiregulin to Neu, ErbB-3, and ErbB-4. J. Biol. Chem. **271**, 20047–20052.

10 Shelly, M., Pinkas-Kramarski, R., Guarino, B. C., Waterman, H., Wang, L. M., Lyass, L., Alimandi, M., Kuo, A., Bacus, S. S., Pierce, J. H. et al. (1998) Epiregulin is a potent pan-ErbB ligand that preferentially activates heterodimeric receptor complexes. J. Biol. Chem. **273**, 10496–10505

11 Karunagaran, D., Tzahar, E., Beerli, R. R., Chen, X., Graus-Porta, D., Ratzkin, B. J., Seger, R., Hynes, N. E. and Yarden, Y. (1996) ErbB-2 is a common auxiliary subunit of NDF and EGF receptors: implications for breast cancer. EMBO J. **15**, 254–264

12 Pinkas-Kramarski, R., Soussan, L., Waterman, H., Levkowitz, G., Alroy, I., Klapper, L., Lavi, S., Seger, R., Ratzkin, B. J., Sela, M. et al. (1996) Diversification of Neu differentiation factor and epidermal growth factor signaling by combinatorial receptor interactions. EMBO J. **15**, 2452–2467

13 Olayioye, M. A., Graus-Porta, D., Beerli, R. R., Rohrer, J., Gay, B. and Hynes, N. E. (1998) ErbB-1 and ErbB-2 acquire distinct signaling properties dependent upon their dimerization partner. Mol. Cell. Biol. **18**, 5042–5051

14 Sweeney, C., Lai, C., Riese, II, D. J., Diamonti, A. J., Cantley, L. C. and Carraway, III, K. L. (2000) Ligand discrimination in signaling through an ErbB4 receptor homodimer. J. Biol. Chem. **275**, 19803–19807

15 Rameh, L. E., Arvidsson, A., Carraway, III, K. L., Couvillon, A. D., Rathbun, G., Crompton, A., VanRenterghem, B., Czech, M. P., Ravichandran, K. S., Burakoff, S. J. et al. (1997) A comparative analysis of the phosphoinositide binding specificity of pleckstrin homology domains. J. Biol. Chem. **272**, 22059–22066

16 Stokoe, D., Stephens, L. S., Copeland, T., Gaffney, P. R. J., Reese, C. B., Painter, G. B., Holmes, A. B., McCormick, F. and Hawkins, P. T. (1997) Dual role of phosphatidylinositol-3,4,5-trisphosphate in the activation of protein kinase B. Science **277**, 567–570

17 Dhillon, A. S., Meikle, S., Yazici, Z., Eulitz, M. and Kolch, W. (2002) Regulation of Raf-1 activation and signaling by dephosphorylation. EMBO J. **21**, 64–71

18 Moelling, K., Schad, K., Bosse, M., Zimmermann, S. and Schweneker, M. (2002) Regulation of Raf–Akt cross-talk. J. Biol. Chem. **277**, 31099–31106

19 Mograbi, B., Bocciardi, R., Bourget, I., Busca, R., Rochet, N., Farahi-Far, D., Juhel, T. and Rossi, B. (2001) Glial cell line-derived neurotrophic factor-stimulated phosphatidylinositol 3-kinase and Akt activities exert opposing effects on the ERK pathway. Importance for the rescue of neuroectodermic cells. J. Biol. Chem. **276**, 45307–45319

20 Rommel, C., Clarke, B. A., Zimmermann, S., Nuñez, L., Rossman, R., Reid, K., Moelling, K., Yancopoulos, G. D. and Glass, D. J. (1999) Differentiation stage-specific inhibition of the Raf–MEK–ERK pathway by Akt. Science **286**, 1738–1741

21 Zimmermann, S. and Moelling, K. (1999) Phosphorylation and regulation of Raf by Akt (protein kinase B). Science **286**, 1741–1744

22 Reusch, H. P., Zimmermann, S., Schaefer, M., Paul, M. and Moelling, K. (2001) Regulation of Raf by Akt controls growth and differentiation in vascular smooth muscle cells. J. Biol. Chem. **276**, 33630–33637

23 Kim, J. H., Saito, K. and Yokoyama, S. (2002) Chimeric receptor analyses of the interactions of the ectodomains of ErbB-1 with epidermal growth factor and of those of ErbB-4 with neuregulin. Eur. J. Biochem. **269**, 2323–2329

24 Resjö, S., Göransson, O., Härndahl, L., Zolnierowicz, S., Manganiello, V. and Degerman, E. (2002) Protein phosphatase 2A is the main phosphatase involved in the regulation of protein kinase B in rat adipocytes. Cellular Signalling **14**, 231–238

25 Obata, T., Yaffe, M. B., Leparc, G. G., Piro, E. T., Maegawa, H., Kashiwagi, A., Kikkawa, R. and Cantley, L. C. (2000) Peptide and protein library screening defines optimal substrate motifs for AKT/PKB. J. Biol. Chem. **275**, 36108–36115

26 Yaffe, M. B., Leparc, G. G., Lai, J., Obata, T., Volinia, S. and Cantley, L. C. (2001) A motif-based profile scanning approach for genome-wide prediction of signaling pathways. Nat. Biotechnol. **19**, 348–353

27 Cohen, B. D., Green, J. M., Foy, L. and Fell, H. P. (1996) HER4-mediated biological and biochemical properties in NIH 3T3 cells. J. Biol. Chem. **271**, 4813–4818

28 Moehren, G., Markevich, N., Demin, O., Kiyatkin, A., Goryanin, I., Hoek, J. B. and Kholodenko, B. N. (2002) Temperature dependence of the epidermal growth factor receptor signaling network can be accounted for by a kinetic model. Biochemistry **41**, 306–320

29 Kholodenko, B. N. (2000) Negative feedback and ultrasensitivity can bring about oscillations in the mitogen-activated protein kinase cascades. Eur. J. Biochem. **267**, 1583–1588

30 Chook, Y. M., Gish, G. D., Kay, C. M., Pai, E. F. and Pawson, T. (1996) The Grb2–mSos1 complex binds phosphopeptides with higher affinity than Grb2. J. Biol. Chem. **271**, 30472–30478

31 Maruta, H. and Burgess, A. W. (1994) Regulation of the Ras signalling network. Bioessays **16**, 489–496

32 Kubicek, M., Pacher, M., Abraham, D., Podar, K., Eulitz, M. and Baccarini, M. (2002) Dephosphorylation of Ser-259 regulates Raf-1 membrane association. J. Biol. Chem. **277**, 7913–7919

33 Garrington, T. P. and Johnson, G. L. (1999) Organization and regulation of mitogen-activated protein kinase signaling pathways. Curr. Opin. Cell Biol. **11**, 211–218

34 Zhou, B., Wang, Z., Zhao, Y., Brautigan, D. L. and Zhang, Z. (2002) The specificity of extracellular signal-regulated kinase 2 dephosphorylation by protein phosphatases. J. Biol. Chem. **277**, 31818–31825

35 Keyse, S. M. (2000) Protein phosphatases and the regulation of mitogen-activated protein kinase signalling. Curr. Opin. Cell Biol. **12**, 186–192

36 Woscholski, R., Dhand, R., Fry, M. J., Waterfield, M. D. and Parker, P. J. (1994) Biochemical characterization of the free catalytic p110α and the complexed heterodimeric p110α. p85α forms of the mammalian phosphatidylinositol 3-kinase. J. Biol. Chem. **269**, 25067–25072

37 Andjelkovic, M., Maira, S. M., Cron, P., Parker, P. J. and Hemmings, B. A. (1999) Domain swapping used to investigate the mechanism of protein kinase B regulation by 3-phosphoinositide-dependent protein kinase 1 and Ser^{473} kinase. Mol. Cell. Biol. **19**, 5061–5072

38 Alessi, D. R., James, S. R., Downes, C. P., Holmes, A. B., Gaffney, P. R., Reese, C. B. and Cohen, P. (1997) Characterization of a 3-phosphoinositide-dependent protein kinase which phosphorylates and activates protein kinase Bα. Curr. Biol. **7**, 261–269

39 Currie, R. A., Walker, K. S., Gray, A., Deak, M., Casamayor, A., Downes, C. P., Cohen, P., Alessi, D. R. and Lucocq, J. (1999) Role of phosphatidylinositol 3,4,5-trisphosphate in regulating the activity and localization of 3-phosphoinositide-dependent protein kinase-1. Biochem. J. **337**, 575–583

40 Andjelkovic, M., Jakubowicz, T., Cron, P., Ming, X. F., Han, J. W. and Hemmings, B. A. (1996) Activation and phosphorylation of a pleckstrin homology domain containing protein kinase (RAC-PK/PKB) promoted by serum and protein phosphatase inhibitors. Proc. Natl. Acad. Sci. U.S.A. **93**, 5699–5704

41 Ivaska, J., Nissinen, L., Immonen, N., Eriksson, J. E., Kahari, V. M. and Heino, J. (2002) Integrin $\alpha 2\beta 1$ promotes activation of protein phosphatase 2A and dephosphorylation of Akt and glycogen synthase kinase 3β. Mol. Cell. Biol. **22**, 1352–1359

42 Downes, C. P., Bennett, D., McConnachie, G., Leslie, N. R., Pass, I., MacPhee, C., Patel, L. and Gray, A. (2001) Antagonism of PI 3-kinase-dependent signalling pathways by the tumour suppressor protein, PTEN. Biochem. Soc. Trans. **29**, 846–851

43 Maehama, T. and Dixon, J. E. (1998) The tumor suppressor, PTEN/MMAC1, dephosphorylates the lipid second messenger, phosphatidylinositol 3,4,5-trisphosphate. J. Biol. Chem. **273**, 13375–13378

44 Tzahar, E., Pinkas-Kramarski, R., Moyer, J. D., Klapper, L. N., Alroy, I., Levkowitz, G., Shelly, M., Henis, S., Eisenstein, M., Ratzkin, B. J. et al. (1997) Bivalence of EGF-like ligands drives the ErbB signaling network. EMBO J. **16**, 4938–4950

45 Biondi, R. M., Cheung, P. C., Casamayor, A., Deak, M., Currie, R. A. and Alessi, D. R. (2000) Identification of a pocket in the PDK1 kinase domain that interacts with PIF and the C-terminal residues of PKA. EMBO J. **19**, 979–988

46 Baulida, J., Kraus, J. H., Alimandi, M., Di Fiore, P. P. and Carpenter, G. (1996) All ErbB receptors other than the epidermal growth factor receptor are endocytosis impaired. J. Biol. Chem. **271**, 5251–5257

47 Mukhopadhyay, S. and Ross, E. M. (1999) Rapid GTP binding and hydrolysis by G_q promoted by receptor and GTPase-activating proteins. Proc. Natl. Acad. Sci. U.S.A. **96**, 9539– 9544
48 Norman, B. H., Shih, C., Toth, J. E., Ray, J. E., Dodge, J. A., Johnson, D. W., Rutherford, P. G., Schultz, R. M., Worzalla, J. F. and Vlahos, C. J. (1996) Studies on the mechanism of phosphatidylinositol 3-kinase inhibition by wortmannin and related analogs. J. Med. Chem. **39**, 1106–1111
49 Ueki, K., Fruman, D. A., Brachmann, S. M., Tseng, Y. H., Cantley, L. C. and Kahn, C. R. (2002) Molecular balance between the regulatory and catalytic subunits of phosphoinositide 3-kinase regulates cell signaling and survival. Mol. Cell. Biol. **22**, 965–977
50 von Gise, A., Lorenz, P., Wellbrock, C., Hemmings, B., Berberich-Siebelt, F., Rapp, U. R. and Troppmair, J. (2001) Apoptosis suppression by Raf-1 and MEK1 requires MEK- and phosphatidylinositol 3-kinase-dependent signals. Mol. Cell. Biol. **21**, 2324–2336
51 Yart, A., Laffargue, M., Mayeux, P., Chretien, S., Peres, C., Tonks, N., Roche, S., Payrastre, B., Chap, H. and Raynal, P. (2001) A critical role for phosphoinositide 3-kinase upstream of Gab1 and SHP2 in the activation of Ras and mitogen-activated protein kinases by epidermal growth factor. J. Biol. Chem. **276**, 8856–8864
52 Heinrich, R., Neel, B. G. and Rapoport, T. A. (2002) Mathematical models of protein kinase signal transduction. Mol. Cell **9**, 957–970
53 Kremmer, E., Ohst, K., Kiefer, J., Brewis, N. and Walter, G. (1997) Separation of PP2A core enzyme and holoenzyme with monoclonal antibodies against the regulatory A subunit: abundant expression of both forms in cells. Mol. Cell. Biol. **17**, 1692–1701
54 Millward, T. A., Zolnierowicz, S. and Hemmings, B. A. (1999) Regulation of protein kinase cascades by protein phosphatase 2A. Trends Biochem. Sci. **24**, 186–191
55 Janssens, V. and Goris, J. (2001) Protein phosphatase 2A: a highly regulated family of serine/threonine phosphatases implicated in cell growth and signalling. Biochem. J. **353**, 417–439
56 Wassarman, D. A., Solomon, N. M., Chang, H. C., Karim, F. D., Therrien, M. and Rubin, G. M. (1996) Protein phosphatase 2A positively and negatively regulates Ras1-mediated photoreceptor development in *Drosophila*. Genes Dev. **10**, 272–278
57 Braconi Quintaje, S. B., Church, D. J., Rebsamen, M., Valloton, M. B., Hemmings, B. A. and Lang, U. (1996) Role of protein phosphatase 2A in the regulation of mitogen-activated protein kinase activity in ventricular cardiomyocytes. Biochem. Biophys. Res. Commun. **221**, 539–547
58 Chaudhary, A., King, W. G., Mattaliano, M. D., Frost, J. A., Diaz, B., Morrison, D. K., Cobb, M. H., Marshall, M. S. and Brugge, J. S. (2000) Phosphatidylinositol 3-kinase regulates Raf1 through PAK phosphorylation of serine 338. Curr. Biol. **10**, 551–554
59 Lynch, D. K. and Daly, R. J. (2002) PKB-mediated negative feedback tightly regulates mitogenic signalling via Gab2. EMBO J. **21**, 72–82
60 Zhang, K., Sun, J., Liu, N., Wen, D., Chang, D., Thomason, A. and Yoshinaga, S. K. (1996) Transformation of NIH 3T3 cells by HER3 or HER4 receptors requires the presence of HER1 or HER2. J. Biol. Chem. **271**, 3884–3890
61 Graus-Porta, D., Beerli, R. R., Daly, J. M. and Hynes, N. E. (1997) ErbB-2, the preferred heterodimerization partner of all ErbB receptors, is a mediator of lateral signaling. EMBO J. **16**, 1647–1655

Received 22 November 2002/7 March 2003; accepted 14 April 2003
Published as BJ Immediate Publication 14 April 2003, DOI 10.1042/BJ20021824